Nonlinear Response and Thermomechanochemical Degradation of a Urethane Elastomer

JOEY MEAD*, SACHCHIDA SINGH, *and* DAVID ROYLANCE

Department of Materials Science and Engineering
Massachusetts Institute of Technology
Cambridge, Massachusetts 02139

and

JACOB PATT

U.S. Army Tank-Automotive Command
Warren, Michigan 48090

We have studied the failure of a urethane elastomer due to cyclic compressive loading, using loading frequencies and specimen sizes for which internal heat generation is an important factor. The eventual failures were generally manifest by internal cracks growing transverse to the loading direction. A variety of experimental analyses indicate that this failure is primarily thermal, in that the temperature rise due to viscous dissipation eventually leads to a melting of the hard segment domains which act to reinforce the material. No strong indication of thermal or thermomechanical bond scission was obtained, although a progressive reduction in the rubbery modulus was noted.

INTRODUCTION

Military tracked vehicles, such as tanks and personnel carriers, use rubber pads on their tracks to reduce road damage, give traction, damp vibrations, and reduce noise. With the high loads and speeds encountered by modern tracked vehicles, the rubber pads often fail in an undesirably short time. Replacement of these pads currently contributes to a substantial portion of the cost of vehicle maintenance. Improving the lifetime of the pad material would help reduce these costs, and this research has been aimed at this goal.

This study was undertaken to investigate the types of damage which occur under repeated cyclic loadings similar to those found in normal service. Under these conditions substantial heat build-up occurs, which in conjunction with the applied stresses have been known to produce a variety of degradation mechanisms in elastomers. Specifically, we have used thermogravimetric analysis (TGA) to characterize the purely thermal degradation process, and compression-compression fatigue to investigate thermomechanical degradation. Physical and chemical changes occurring during fatigue were monitored by differential scanning calorimetry (DSC), swelling in dimethyl formamide, dynamic mechanical spectroscopy, and infrared spectroscopy.

Our study shows that given sufficient load cycling, urethane specimens can fail by cracks generated at their centers. DSC analysis showed an increased hard segment transition temperature due to thermal annealing effects. All samples had a decreased elastic modulus (E') after fatigue, which may be due to a stress-softening mechanism analogous to the Mullins effect. Only one block tested showed any significant changes in crosslink density as determined by swelling analysis, but this singular measurement may have been due to a processing irregularity (for example, an exotherm during cure might lead to degradation of the material). The main failure mechanism appears to be softening of the hard segment followed by rupture. The cracks appear at the center of the block, which is the hottest area, supporting this mechanism.

MATERIALS

Cast urethane elastomer systems, such as the one used in this study, are generally prepared by the reaction of an isocyanate terminated

* Present address: Army Materials Technology Laboratory, Watertown, MA 02172

Reprinted from POLYMER ENGINEERING AND SCIENCE, JANUARY, 1987, Vol. 27, No. 2

prepolymer with a low molecular weight curative such as a diol or diamine. The prepolymer is usually prepared by end-capping a polyether or a polyester with a diisocyanate, forming a urethane bond and leaving two free isocyanates, which can be further reacted (1). Next, the prepolymer is reacted with a "curative". If a diol is used, a polyurethane is formed. If a diamine is reacted, a polyurethane urea is formed. When an excess of isocyanate is used crosslinking may occur through the formation of allophanates or biurets, with the biuret reaction occurring more rapidly than the allophanate reaction (1). Urethanes formed in this manner are usually two-phase systems, in which the polyether or polyester forms a domain of aggregated "soft segments," and the isocyanate and curative form hard segment domains. These hard segments act as physical crosslinks, often enhancing the physical properties of the polymer.

The material chosen for this study was a commercial polyether polyurethaneurea system, prepared from a toluene diisocyanate (TDI) prepolymer and a diamine curative, trimethylene glycol-di-p-amino benzoate. The stoichiometry (curative/polymer weight ratio) used was 85 percent. This material has shown good wear resistance in rough-terrain track testing, and is a possible replacement for more traditional rubber compounds. Further, the urethane is not so highly compounded as the traditional carbon-black filled elastomers, and this simplifies many of the analytical techniques needed for its analysis.

Molded blocks were prepared by the following method. The diamine curative and prepolymer were weighed into separate beakers filled with argon gas and covered with aluminum foil to reduce the exposure of the contents to atmospheric moisture. An extra gram of curative was included to compensate for the loss that occurred during pouring. The prepolymer was heated in a 100°C oven and the curative (m.p. 140°C) was melted in a 150°C oven. The curative was then degassed and returned to the oven, then the molten prepolymer was degassed and allowed to cool to 90°C. The curative was removed from the oven, poured into the beaker containing the prepolymer, and mixed quickly with a wooden dowel. Complete mixing required about 20 s. The polyurethane mixture was then degassed for approximately two min. The polymer was quickly poured down the stirring rod into a preheated mold (100°C), which had been sprayed with a silicone mold release. After filling the mold, the specimen was placed in a 100°C oven for 45 min before demolding. The block was returned to the oven and allowed to cure at 100°C for four to five h. The blocks were aged for two weeks at room temperature before testing. Four blocks molded by the manufacturer were also tested.

Several problems can arise during polymer preparation because of the short working pot life of four min and the low prepolymer preheat temperature relative to the melting point of the curative. When the prepolymer is not heated to a sufficiently high temperature, the curative will solidify, producing small curative flakes throughout the specimen. In the initial attempts at specimen preparation this problem produced blocks with incorrect stoichiometry, as well as reduced properties because of the crack initiation sites in the curative flakes. With the prepolymer and/or curative at too high a temperature, the pot life of the polyurethane is reduced due to the increased reaction rate of the components at higher temperatures. This results in premature gelation, with the reaction mixture solidifying in the beaker rather than the mold.

The cure temperature can affect the properties of the elastomers, and the exotherm during cure may cause the properties of the center of the specimen to vary from the outside portions. As discussed in *Ref. 1*, Fujioko and Goto have shown that a polyurethane prepared from toluene diisocyanate (TDI), polyoxypropylene glycol (PPG), and 3,3'-dichloro-4,4'-diaminodiphenylmethane (MOCA) exhibits decreased hardness, tensile strength, and elongation as the cure temperature is raised above 100°C. This was attributed to the increased formation of biuret groups above 100°C. The biuret groups were felt to disrupt the interchain forces leading to a reduction in modulus, even though an increase in crosslink density, for a conventional rubber, would be expected to increase the modulus. In fact, crosslink formation has been reported to cause an anomalous decrease in the modulus (2). In the studies of Pigott, *et al.* (2), where the crosslink density in the hard segment was changed by adding different amounts of trimethylol propane during chain extension to a polyester polyurethane, the modulus was found to decrease, then increase, as the crosslink density was changed.

EXPERIMENTAL RESULTS

Cyclic Loading

A servohydraulic Instron model 1331 was used to apply compression-compression sinusoidal cyclic loading at a frequency of 6.5 Hz and a 0.1 ratio of minimum to maximum stress. The specimens were tested between two parallel flat plates, using double-stick tape to prevent the block from slipping out of the test machine. The tape also inhibits lateral motion of the loaded surfaces, which produces a barrelling of the test specimen during loading. The barrelling in turn generates a complicated and nonuniform stress state within the specimen. The testing was done in load control mode on the Instron, because it was felt this would more accurately simulate tank track pad conditions. The temperature of the blocks was monitored by a thermocouple which had been inserted in a hole drilled to the center of the block.

The results of the loading test are summarized in *Fig. 1*, which shows the lifetime or test duration *vs.* maximum stress for each of the specimens tested. The failure mode was via cracks generated at the center of the test block. Some specimens were loaded to failure, while some tests were stopped short of failure and the specimens removed to analyze the degradation process. The testing we have done is not fatigue testing in the usual sense due to the small number of blocks examined. The extensive analysis required for each block, in order to determine the failure mechanism, limited the total number of blocks that could be tested.

All the blocks were 63.5 by 63.5 by 63.5 mm with the exception of two commercially prepared blocks, which were 63.5 by 63.5 by 76.2 mm. The larger blocks were tested with the same cross-sectional area under load at a maximum stress of 6.62 MPa. One specimen was taken to failure and the other test was stopped before failure occurred. A third commercially prepared block, 63.5 by 63.5 by 63.5 mm, was tested at 4.96 MPa maximum stress. This specimen reached an equilibrium temperature of 91°C, and the test was stopped at 2.1×10^6 cycles without failure.

A typical thermal history is shown in *Fig. 2*, which plots temperature *vs.* number of cycles for the three specimens tested at 6.62 MPa. The internal temperatures of all specimens showed a continuous rise with increasing load cycles, with the exception of the specimen tested at the lowest stress (4.96 MPa); this appeared to reach an equilibrium between internal heat generation and surface convective losses which produced a constant temperature. In general, the temperature histories indicate that the internal temperatures at failure approach 180°C.

Thermogravimetric Analysis

We conducted a series of thermogravimetric analyses in order to assess the extent to which purely thermal degradation mechanisms might contribute to the failure of the loaded specimens. Thermal degradation would be expected to lead to decreased crosslink density and molecular weight, changing the mechanical and thermal properties of the polyurethane. Thermogravimetric analysis (TGA) records of weight loss *vs.* temperature were obtained using a DuPont 1090 at a heating rate of 10°C/min in a nitrogen atmosphere. The TGA trace for unfatigued material is shown in *Fig. 3*.

It was generally observed that for our study materials no weight loss occurs before 250°C. Since the specimens subjected to cyclic loading fail well before this temperature is reached, it seems likely that the thermal degradation reactions observed by TGA are not involved in the failure of the loaded blocks. Since the TGA monitors only those reactions leading to volatilization and weight loss, this does not exclude the possibility that other thermal degradation reactions, not producing volatile products, are involved in the failure process.

Differential Scanning Calorimetry

Polyurethane block copolymers are generally two-phase systems, but they can exhibit a substantial mixing of soft segments in the hard domains, and vice versa. The degree of this phase mixing will affect the transition temper-

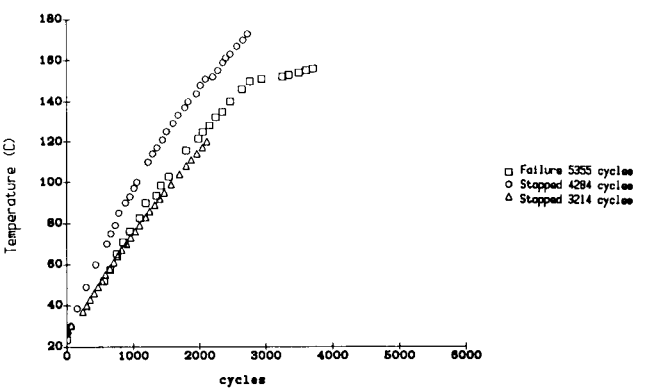

Fig. 2. Internal temperature histories of three different specimens tested at 6.62 MPa maximum stress.

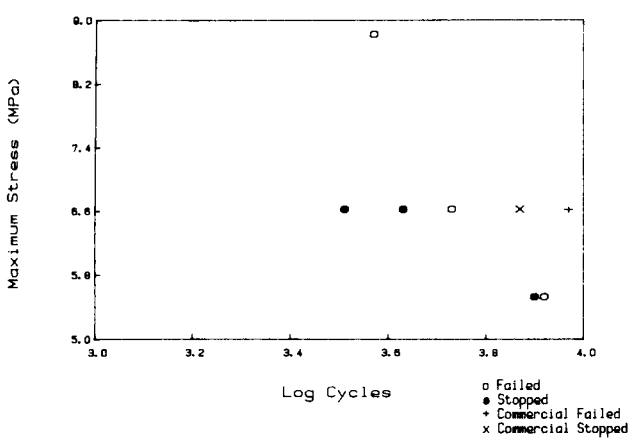

Fig. 1. Summary of load cycling tests: cycles to failure or termination of test. "Commercial" specimens prepared by Polaroid, others by us.

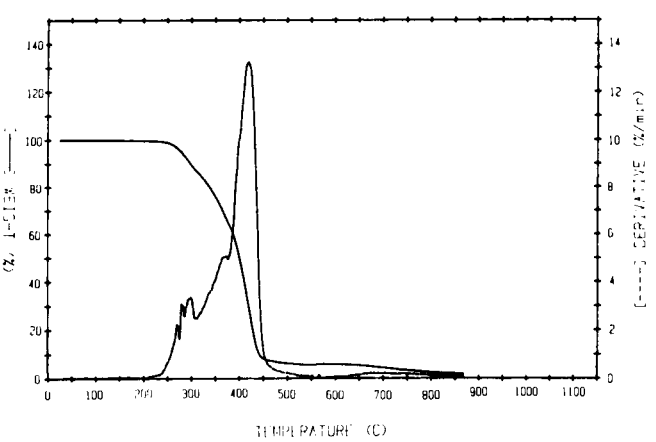

Fig. 3. Thermogravimetric analysis in nitrogen. Solid line is percentage of weight remaining; dotted line shows rate of weight loss.

atures of both hard and soft segments, and phase mixing has been used to explain the increase in soft segment T_g with increasing hard segment content (3). Reasoning that alterations in phase morphology might be involved in the failure of loaded blocks, we used differential scanning calorimetry (DSC) to study the transition temperatures of unfatigued and fatigued specimens.

DSC analyses were conducted using a Perkin-Elmer DSC IV with a heating rate of 10°C/min. A comparison of typical DSC scans for unfatigued and fatigued material is shown in *Fig. 4*. There appear to be two high temperature transitions in the unfatigued material, one occurring near 180°C, and the other near 205°C. Specimens which had been loaded to failure show only one transition, which is at nearly the same temperature as the higher temperature transition for the unfatigued material.

A plot of the transition temperature after fatigue (the lowest value for those showing two transitions) *vs.* fatigue cycles is shown in *Fig. 5* for specimens fatigued at 6.62 MPa maximum stress. As can be seen, there are no changes in the transition temperature with the specimen

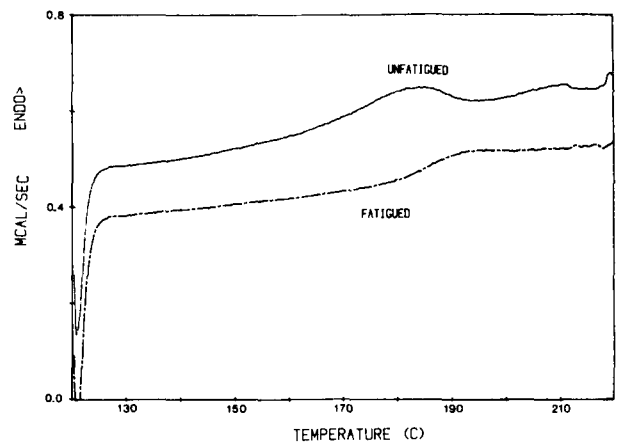

Fig. 4. Typical DSC traces showing the increase in hard segment transition temperature with fatigue. Specimen fatigued at 8.82 MPa maximum stress to failure.

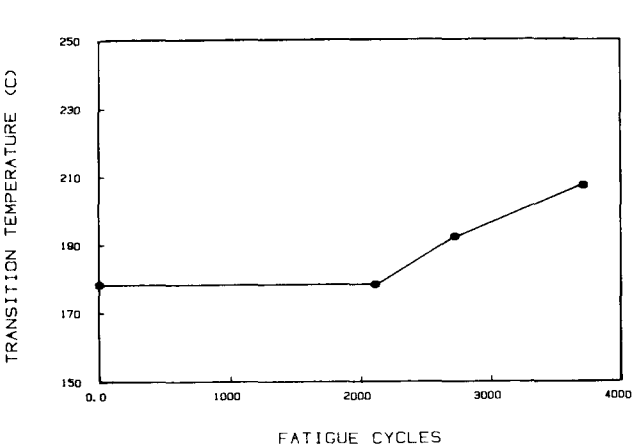

Fig. 5. Effect of increasing fatigue cycles on hard segment transition temperature (lowest value shown for specimens having two transitions) for specimens fatigued at 6.62 MPa maximum stress.

fatigued to 2,110 cycles (120°C maximum internal temperature), after which there is a continuous increase in the transition temperature with the number of fatigue cycles until specimen failure.

The increase in transition temperature with load cycling may be due only to thermal annealing, because heating samples in the DSC also moves the lower temperature transition upward. Of course, the high temperatures generated in the loading tests might be expected to produce similar effects. The transition shift may be due to an increase in the amount of phase separation, or an improved ordering in the hard segment domains. Both these phenomena would increase the hard segment T_g. Since no improved order after annealing was reported in similar systems (4), increased phase separation may be the most viable explanation. This conclusion is tentative because if this were the case we would expect the T_g of the soft segment to change as well. This was not observed in the DSC analyses.

Cain (5) studied a polyurethane system very similar to ours, prepared from polytetramethylene ether glycol (PTMEG), TDI, and 3,3′-dichloro-4,4′-diaminodiphenylmethane (MOCA), and found the presence of two high temperature transitions. Annealing either moved the lower transition upwards or caused it to disappear. With the aid of IR measurements at high temperatures, Cain was able to correlate the transitions to hydrogen bonding in the urethane carbonyls (lower temperatures) and urea carbonyls (higher temperatures). It is quite reasonable that our system shows similar behavior. Although we cannot be exactly sure what changes occur to the hard segment structure after annealing, we conclude that the changes seen in the DSC scans after fatigue are the result of thermal treatment at the high temperatures observed during testing.

Swelling Studies

We have explored a number of approaches to monitoring the molecular mechanisms underlying the thermomechanical degradation of the loaded blocks. None of these have been simple due to the intractable nature of the material and the relatively dilute concentration of molecular scission events. One possible approach is to measure changes in crosslink density (ν_e/V). This parameter influences a number of physical properties, most notably the glass transition temperature, the rubbery modulus, and the uptake of certain swelling fluids.

The crosslink density can be computed from solvent uptake measurements by means of the Flory-Rehner equation:

$$\frac{\nu_e}{V} = -\frac{1}{V_s} \times \frac{\ln(1 - v_r) + v_r + \chi v_r^2}{v_r^{1/3} - 2v_r/f} \qquad (1)$$

ν_e/V is the crosslink density (mole/cm^3), V_s is

the molar volume of the solvent, χ is the polymer-solvent interaction parameter, v_r is the volume fraction of rubber in the swollen sample, and f is the functionality of the crosslink. v_r can be calculated by the weight of the specimen while swollen and after removal of the solvent, if the density of the polymer and solvent are known.

Since the interaction parameter χ was not known for our polymer-solvent system, we sought an independent measure of the crosslink density by which the parameter could be inferred from the Flory-Rehner equation. For this purpose we measured the elastic modulus of swollen specimens, using a swelling solvent (dimethylformamide, DMF) which disrupts the hard segment domains. The crosslink density is given in terms of the elastic modulus by (7):

$$\nu_e/V = Fv_r^{1/3}/\{ART(\alpha - \alpha^{-2})\} \qquad (2)$$

where ν_e/V is the moles of effective network chains per unit volume of polymer, F is the force to obtain an extension, α, v_r is the volume fraction of elastomer in the swollen specimen, A is the unswollen cross-sectional area, R is the gas constant, and T is the temperature. This value of the crosslink density can then be used in the Flory-Rehner equation to calculate χ.

To verify that the DMF solvent breaks up the hard segment hydrogen bonding to allow measurement of the primary crosslink density, we immersed specimens with (85 percent stoichiometry) and without (100 percent stoichiometry) biuret crosslinks in DMF. The uncrosslinked material completely dissolved in the solvent, while the crosslinked material was only swollen. This indicates that DMF does disrupt the hard segment domain structure.

For swelling measurements, specimens weighing approximately 0.4 grams were placed in 80 ml of DMF and allowed to swell for 25 h at 25°C. The specimens were removed and weighed in sealed jars. The deswollen weight was obtained by drying the specimens in a 60°C vacuum oven overnight. Conventional stress-strain tests were then conducted on the swollen tensile specimens, and the crosslink density was calculated by *Eq 2*. Finally, this result was used in the Flory-Rehner equation to compute the χ value; we obtained $\chi = 0.468$.

The χ value obtained above was used in the Flory-Rehner equation to compute the crosslink densities in blocks before and after fatigue loading. The unfatigued material exhibited a mean value of 1.53×10^{-4} mole/cm^3 and a standard deviation of 6.98×10^{-5}. The corresponding average values for all specimens loaded to failure was 2.33×10^{-4} moles/cm^3 with a standard deviation of 1.17×10^{-4}. Only one specimen showed a decreased crosslink density after fatigue. It may be that this block was different from the others, perhaps the starting materials had been degraded in some way, or the processing conditions were different.

We conclude from the swelling experiments that no significant permanent chain scission is required for failure of polyurethane elastomers under compression loading. Of course, bond scission must occur at least near the free surfaces created when the specimen finally fails through crack growth, but we feel we can rule out the sort of extensive and global bond dissociation which has been observed by electron spin resonance in some other polymers (8).

Infrared Spectroscopy

While thermogravimetric and swelling analyses show no evidence of molecular rearrangements during loading, these tests are ambiguous in some respects. To explore further the possibility of reactions during loading, we conducted infrared spectroscopic analysis of the unfatigued and fatigued material. Attenuated total reflectance (ATR) spectra were obtained using a Digilab FTS-IMX. This method was chosen because the material was insoluble and could not be cast into a film.

Figure 6 shows the IR spectra for unfatigued and fatigued materials. The expected degradation reaction, based on the literature (9, 10), is the dissociation of the urethane and urea bonds to form isocyanates and alcohols or amines.

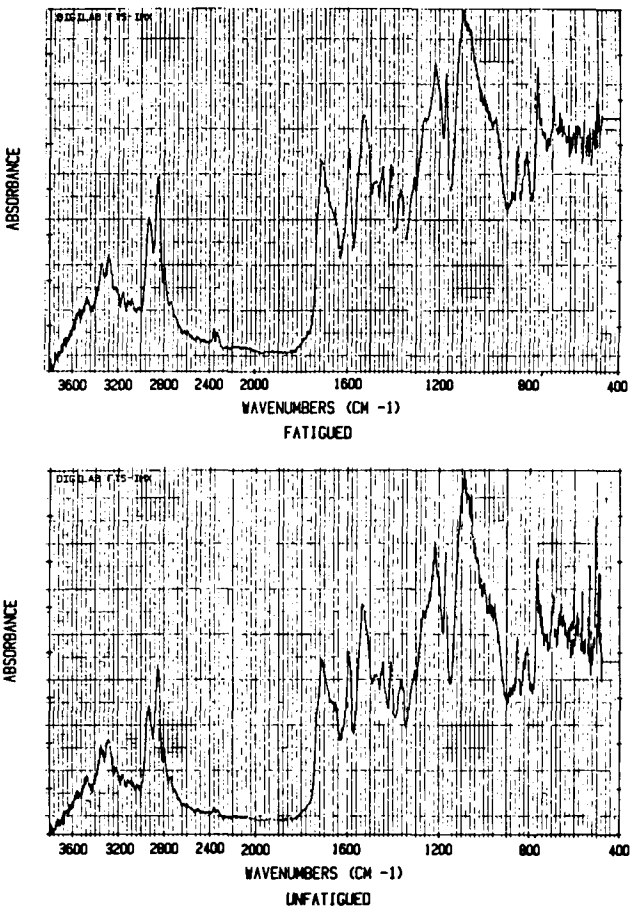

Fig. 6. Influence of fatigue on FTIR Spectra for material fatigued at 5.52 MPa maximum stress to failure. Top spectrum fatigued; bottom spectrum unfatigued.

There are no new peaks for isocyanates, amines, or alcohols in the spectrum for the fatigued material, thus permanent rupture of the urethane and urea bonds does not appear to occur during fatigue cycling. There are no new peaks, nor increases in the carbonyl region, which might indicate oxidation reactions. This is not unexpected because the concentration of oxygen present at the center of the block is likely to be small. There are essentially no changes in the IR spectrum after fatigue, supporting the premise that the failure mechanism involves only localized mechanical degradation of the specimen, without extensive mechanochemical reactions.

There is still the possibility that reversible reactions could occur at high temperature, whose absorption bands vanish when the specimen is cooled and the spectra taken at room temperature. For example, the urethane bonds could rupture at high temperature and subsequently reform after the sample is cooled. To investigate the probability of these reactions, high temperature infrared spectroscopy was run under an inert atmosphere. *Figure 7* shows the IR spectra with increasing temperature. No changes appear in the spectra for temperatures up to 240°C, which is well above the temperatures encountered at specimen failure. These data show no evidence of any reactions which might occur at high temperature during the fatigue process but reverse upon cooling.

Dynamic Mechanical Analysis

The dynamic mechanical spectrum of two-phase urethane elastomers shows two principal relaxations. The first, at approximately −30°C, is the glass transition of the soft segment domains, and corresponds to a large reduction in modulus from a glassy to a rubbery plateau. With crosslinking this plateau region is extended. At sufficiently high temperature—approximately 180°C—the hard segment reinforcing domains melt (11); this allows the urethane to become fluidlike and is the basis for thermoplastic elastomer technology. The hard segment melting would be expected to mark the upper service temperature of these materials.

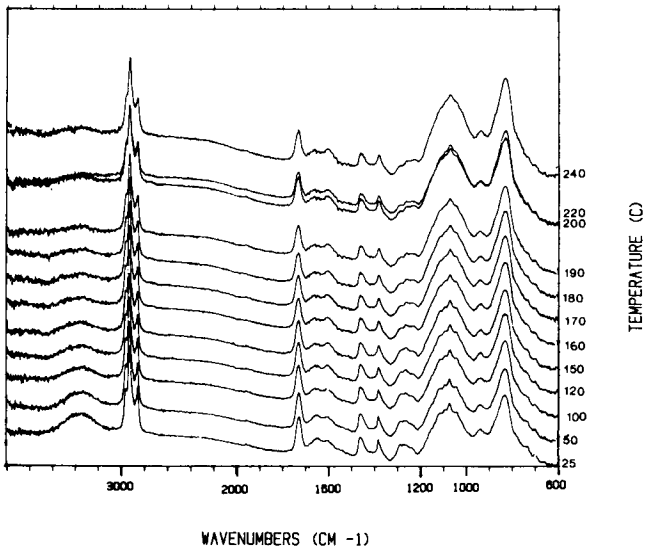

Fig. 7. Analysis of polyurethane at high temperatures by infrared spectroscopy. No evidence for reversible bond dissociation.

The elastic modulus in the rubbery plateau region can be used to determine the crosslink density through the well-known equations of rubber elasticity. The appropriate stress-strain relation is (12):

$$f = E/3(\alpha - \alpha^{-2}) \tag{3}$$

where f is the force per unit unstrained cross-sectional area, E is the Young's modulus, and α is the elongation. Assuming incompressibility and setting Poisson's ratio to 0.5, then (12):

$$E = 3G = 3RT(\nu_e/V) \tag{4}$$

This relation allows us to determine the crosslink density from a measurement of the rubbery modulus. The approach is similar to that used earlier in determining the crosslink density for the purpose of obtaining a suitable solvent interaction parameter.

An Autovibron dynamic mechanical analyzer was used for measurement of the elastic modulus. This system uses the basic Rheovibron DDV-II (Toyo Baldwin Co.), but includes an automation package (Imass, Inc.). The dynamic properties were measured at a frequency of 110 Hz from −130 to 150°C. Fatigued specimens were microtomed from sections taken from the center of the test specimen, as close to the cracks as possible.

All the values for crosslink density calculated by this method are higher than by swelling analysis. This is not unexpected since the modulus measurements include the reinforcing effect of the hard segment of domains, while these domains were dissolved in the swelling solvent. The rubbery modulus decreases with increasing temperature, indicating that ideal rubber elasticity is not attained (13), possibly due to internal energy contributions. However, these data may still give an approximate estimate of the crosslink density.

Figure 8 compares the elastic moduli for specimens fatigued at 6.62 MPa maximum stress. As can be seen, the modulus values above the soft segment glass transition show a progressive decrease with number of fatigue cycles, even though the swelling measurements showed no change with fatigue.

The reduction in rubbery modulus with increasing loading cycles is shown in *Fig. 9* for specimens fatigued at 6.62 MPa maximum stress. This modulus reduction clearly indicates some type of permanent change. Thermal annealing tests showed no permanent change in the elastic modulus, indicating that high temperatures alone do not produce these changes.

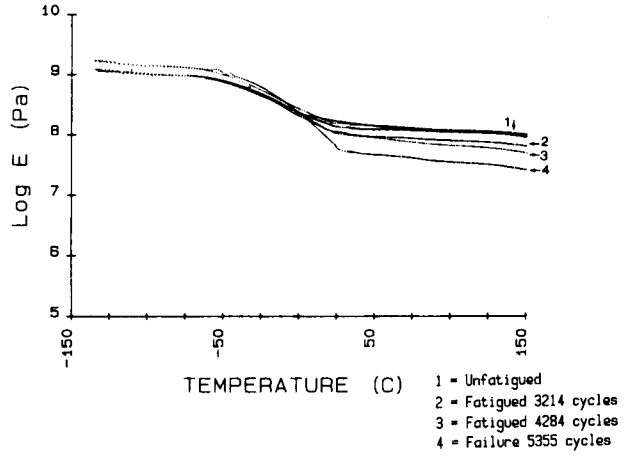

Fig. 8. Effect of fatigue cycles on elastic modulus (E') curves (6.62 MPa maximum stress).

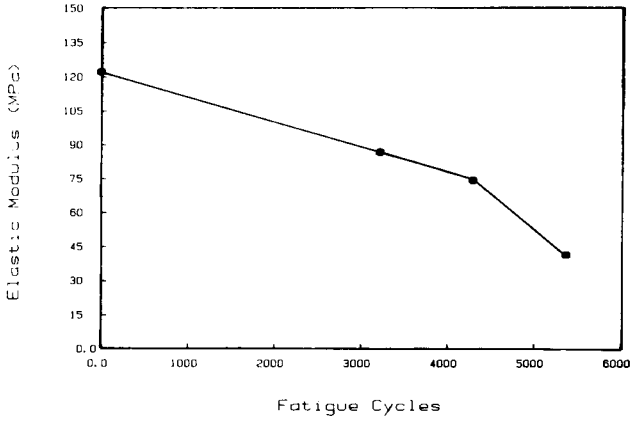

Fig. 9. Reduction of elastic modulus with fatigue cycles for specimens fatigued at 6.62 MPa maximum stress.

A possible explanation for this modulus reduction is a type of "Mullins Effect", which was originally found in filler-loaded rubbers, but has since been found in polyurethane elastomers (14). Trick (14) found a reduction in modulus with repeated extension, although in his case almost all of the reduction occurred in the first cycle. The stress-softening phenomenon is believed to be caused by the disruption of the glassy domains under repeated stretching (15).

Kaneko, *et al.* (16) studied the cut growth fatigue of polyurethanes prepared from PTMEG, TDI, MOCA, and hexamethylene diisocyanate (HMDI). After constant load fatigue they measured the changes in elastic modulus with the Rheovibron. For all fatigued samples a decrease in the elastic modulus was encountered, but the authors did not investigate if the amount of change was dependent on the number of fatigue cycles. Kaneko, *et al.* suggested that the differences they noted after fatigue could be due to orientation under stress.

Either orientation or disruption of the hard domains is a possible explanation for the changes seen in compression fatigue tests. The changes seen in the modulus are clearly not caused by high temperatures alone, but require the application of stress. For the specimen tested at 4.96 MPa, which was cycled at low load levels with little heat build-up, the modulus values show only a very slight reduction. This indicates that stress alone does not produce the modulus reduction, but rather a combination of both stress and heat build-up. The continuous increase in temperature leads to softening of the material, which in turn causes increased deformation in load-controlled tests. This increased deformation amplitude will lead to continued softening (15). The increasing temperature causes stress softening throughout the test, rather than mainly in the first cycle. Thus, we can expect the material properties of polyurethanes to change continuously as fatigue degradation occurs.

High Temperature Mechanical Properties

The dynamic mechanical spectroscopy reported above was useful in fingerprinting the overall nature of the urethane response and for computing the crosslink density from the rubbery modulus. However, these dynamic tests did not extend into the range of temperatures above approximately 150°C, where the failures of the loaded blocks were observed to occur.

A special gripping system was required to conduct tests at these higher temperatures, because samples ruptured at the grips when the material softened. The gripping system devised is as follows: precut specimens were glued on end to two small copper tabs with epoxy. The epoxy was allowed to cure overnight at room temperature. Two pieces of sandpaper were wrapped around the copper tabs, then the sample was placed in the Autovibron and run from room temperature to 250°C. A sample of the epoxy glue was cast onto the tabs and run in the Autovibron to distinguish any transitions for the epoxy. The absolute modulus values may be incorrect because of the tabbing system, but only the transition temperatures were of interest for this section of the work.

The elastic moduli (*E'*) for the polyurethane (using the new gripping system) at two different frequencies are compared with the epoxy alone in *Fig. 10.* For the polyurethane a small transition is seen near 75°C, and a very large drop in modulus is found beginning near 175°C. By comparing the elastic moduli for the epoxy with the polyurethane data, we can assign the transition at 75°C to the epoxy. Further proof for this lies in the fact that this transition was never seen in polyurethane runs without the special gripping system. The epoxy elastic modulus remains essentially constant from 100 to 250°C. Therefore, the transition beginning at 175°C is the hard segment transition. This transition temperature correlates well with the hard segment transition temperature of 180°C found by DSC measurements.

Fatigue failure occurs near 200°C, which is in the range where the elastic modulus is se-

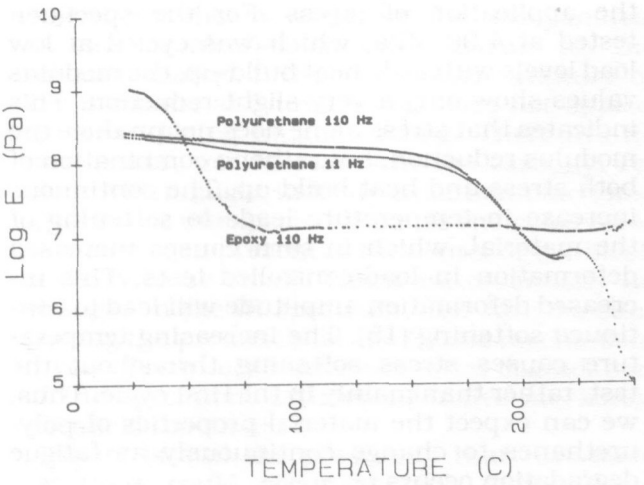

Fig. 10. Elastic modulus at high temperatures for epoxy and polyurethane, showing the loss of stiffness at urethane hard segment transition.

verely reduced. Softening of the material at these temperatures leads to rupture under the high deformations encountered during compression fatigue.

DISCUSSION

The failure mechanism under compressive loading is a consequence of the complicated and nonuniform stress distribution experienced by the block specimens. We are currently performing finite element analysis studies of this aspect of the problem, but in the meantime it is possible to outline the salient features of the stress state using previously published reports.

For blocks which are bonded to end plates, the applied force can be viewed as being composed of two portions: one part is responsible for the surface displacement in the loading direction, and for perfectly lubricated load surfaces would be accompanied by a lateral Poisson displacement of the specimen. Since for bonded plates the surfaces are constrained against lateral motion, a shear displacement can be superposed to restore points on the rubber surface to their original positions (17). For a linearly elastic, incompressible, and isotropic material the hydrostatic pressure component of the stress has a maximum at the center and a parabolic decrease towards the outside. As the height of the block increases the maximum internal pressure decreases (18). When the thickness of the block increases the effect of the constrained surfaces (shear forces) will contribute less to the stress distribution in the block (18).

Reed and Thorpe (19) determined the shear stresses in a compressed block by finite element analysis. The shear stresses were found concentrated in the top outside corners and negligible at the center. Therefore, although there may well be some small amount of shear stresses at the center of the block, their contribution to the failure mechanism is likely to be small.

For a compressed sample with frictionless surfaces, Treloar (20) states the equilibrium strain in a compressed block is the same as the equilibrium strain for a specimen biaxially strained perpendicular to the loading direction. For Treloar's case no bulging effects occur as in our test.

Under fatigue all blocks taken to failure exhibit cracks formed at the center of the specimen. These cracks run perpendicular to the loading direction. *Figure 11* shows the internal cracks, generated during fatigue testing, on a cut section of one of our specimens. *Figure 12* shows the internal cracks for a clear polyurethane of a different composition than our specimens. The internal cracks occur in specimens tested without thermocouples, indicating that the insertion of a thermocouple does not change the mode of failure, although it undoubtedly produces stress concentrations.

Buckley (21) conducted compression tests on cylindrical specimens of styrene-butadiene rubber in a Goodrich Flexometer. He found a similar type of failure, with internal and/or external cracks running perpendicular to the loading direction. Although Buckley felt the stress state in his test would be much more complex than Treloar described for uniaxial compression, Buckley suggested the observed failures could be due to biaxial extension. The strains in the center of the specimen would be similar to a flat sample extended in two directions. The model which Buckley used to describe his failures is shown, with changes to represent a square cross-sectional surface as in our specimens, in *Fig. 13.*

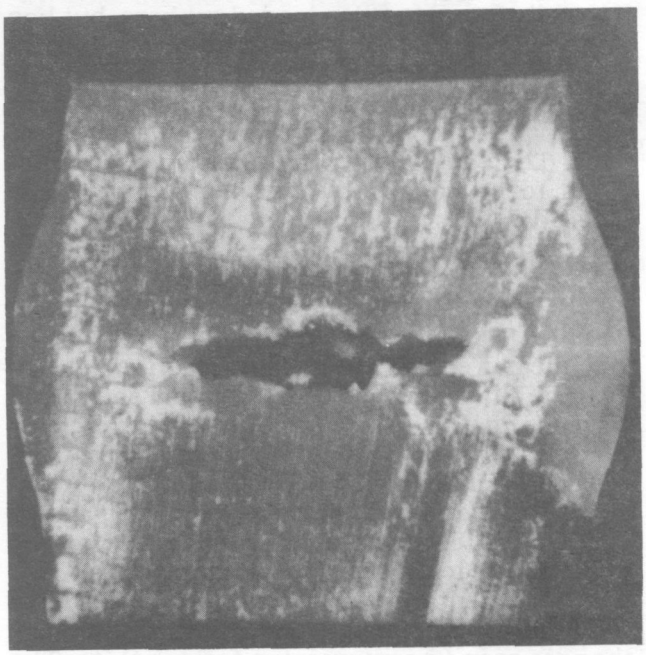

Fig. 11. Specimen cut open to reveal internal center cracks after failure. Loading direction perpendicular to cracks.

Fig. 12. Uncut specimen showing internal cracks.

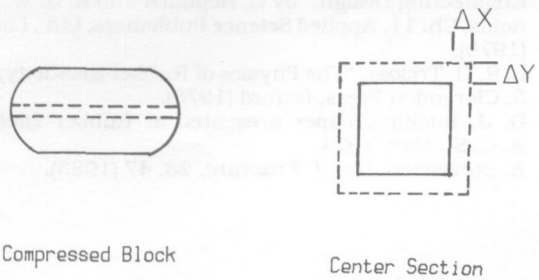

Fig. 13. Biaxial tension model of a compressed block. Left diagram is side view of a compressed block exhibiting bulging. Right diagram is top view of a center slice showing extension of the elastomer perpendicular to loading direction.

In this model the compressed specimen exhibits bulging. A slice taken from the center of the specimen, perpendicular to the loading direction, shows extensions similar to those of a biaxially stretched sample. These extensions are believed to cause biaxial tensile failure of the specimen (21).

Recently, Stevenson (22) studied the formation of cracks in bonded rubber blocks. He found cracks to initiate at the bonded surfaces under tensile stress concentrations. In contrast to Buckley's results, he found no evidence for much heat build-up or internal cracking.

The results of our testing correlate well with the experiments of Buckley. It may be that heat build-up changes the characteristics of the failure so that only internal cracking initiates the failure, with external cracking appearing only at the very end of the test. Under compression cycling heat build-up occurs; the hottest portion of the specimen being the center of the block. The center portion of the block is subjected to extensional strain, and as the temperature at the center of the block approaches the hard segment transition temperature, the material properties at the center of the specimen will degrade. This weakening of the center portion of the specimen, in conjunction with the extensional strain, causes failure at the center of the specimen.

CONCLUSIONS

Under sufficiently high load amplitude, urethane blocks failed by cracking at the center of the test specimen. Thermochemical degradation reactions do not appear implicated in this process, since TGA traces showed weight loss beginning at 250°C, well above the maximum temperatures recorded at fatigue failure. DSC analysis showed an increased hard segment transition temperature, apparently caused by thermal annealing at the high temperatures of the fatigue test.

Swelling analysis indicated that no significant breakdown in crosslink density is required for failure of specimens in compression loading. There is scant experimental evidence for chain scission and essentially no evidence by infrared measurements that the urethane and urea bonds dissociate at high temperatures and subsequently reform as the material is cooled.

All samples had a decreased elastic modulus (E') after fatigue; this reduction continues with increasing number of loading cycles. The internal temperature also increases with the number of cycles, and this leads to softening of the material and increased deformation. Stress-softening continues with increased amplitude of deformation, so the modulus decreases throughout the duration of the test. The modulus reduction is not caused by mechanical stress or thermal annealing alone, but requires the interaction of both.

Under compression cycling heat build-up occurs; the hottest portion of the specimen is at the center of the block. This central portion also is subjected to extensional strain, and as the temperature at the center of the block approaches the hard segment transition temperature, the modulus of the material decreases dramatically. This leads to higher and higher extensions, and finally, rupture of the specimen. This weakening of the center portion of the specimen, in conjunction with the extensional strain, causes failure at the center of the specimen, rather than surface failure initiation.

From this work it seems that the hard segment transition temperature determines the lifetime of a cyclically compressed polyurethane block. For long part lifetimes the polyurethane must possess a very high temperature hard segment transition, or the heat build-up characteristics of the material must be such that the service temperature of the part is well below the hard segment transition.

ACKNOWLEDGMENTS

The authors gratefully acknowledge the support of this work by the U.S. Army Tank-Automotive Command under contract DAAE07-83-K-R013. We also wish to thank Preston Kemp and Linda VanDuyne, undergraduate assistants, and Kenneth Scott and Cal Harmon of Goodyear for providing technical assistance. Dominick Finocchio and Theodore Jula of Polaroid were extremely helpful in providing materials and technical discussion. Finally, we were most fortunate to have the technical assistance of the Army Materials and Mechanics Research Center in performing several of the analyses discussed here. In particular, the authors would like to thank James Sloan, Emily McHugh, Judy Yeaton, Rebecca Jurta, Gary Foley, Margaret Roylance, and William Houghton.

REFERENCES

1. G. Trappe, "Relations Between Structures and Properites of Polyurethanes," in "Advances in Polyurethane Technology," Ed. by J. M. Buist and H. Gudgeon, Ch. 3, John Wiley & Sons, Inc., New York (1968).
2. K. A. Pigott, B. F. Frye, K. R. Allen, S. Steingiser, W. C. Darr, and J. H. Saunders, *J. Chem. Eng. Data*, **5**, 391 (1960).
3. C. S. P. Sung and N. S. Schneider, *Macromolecules*, **8**, 68 (1975).
4. N. S. Schneider, C. S. P. Sung, R. W. Matton, and J. L. Illinger, *Macromolecules*, **8**, 62 (1975).
5. A. R. Cain, W. R. Conard, S. E. Schonfeld, and B. H. Werner, *Am. Chem. Soc., Div. Polym. Chem. Polym. Prepr.*, **17**, 580 (1976).
6. E. T. Bishop and S. Davison, *J. Polym. Sci. - Part C*, **26**, 59 (1969).
7. E. F. Cluff and E. K. Gladding, *J. Appl. Polym. Sci.*, **3**, 290 (1960).
8. D. Roylance, "Characterization of Polymer Deformation and Fracture," "Applications of Polymer Spectroscopy," Ch. 13, Academic Press, New York (1978).
9. J. H. Saunders and J. K. Backus, *Rubber Chem. Technol.*, **39**, 461 (1966).
10. A. Ballisteri, S. Foti, P. Maravigna, G. Montaudo, and E. Scamporrino, *J Polym. Sci.: Polym. Chem. Ed.*, **18**, 1923 (1980).
11. S. L. Cooper and A. V. Tobolsky, *Textile Res. J.*, **36**, 800 (1966).
12. G. Allen, P. L. Edgerton, and D. J. Walsh, *Polymer*, **17**, 65 (1976).
13. T. L. Smith and A. B. Magnusson, *J. Polym. Sci.*, **42**, 391 (1960).
14. G. S. Trick, *J. Appl. Polym. Sci.*, **3**, 252 (1960).
15. S. L. Cooper, D. S. Huh, and W. J. Morris, *Ind. Eng. Chem. Prod. Res. Dev.*, **7**, 248 (1968).
16. Y. Kaneko, Y. Watabe, T. Okamoto, Y. Iseda, and T. Matsunaga, *J. Appl. Polym. Sci.*, **25**, 2467 (1980).
17. A. N. Gent and E. A. Meinecke, *Polym. Eng. Sci.*, **10**, 48 (1970).
18. B. P. Holownia, *J. Strain Analysis*, **7**, 236 (1972).
19. A. J. Reed and J. Thorpe, in "Elastomers: Criteria for Engineering Design," by C. Hepburn and R. J. W. Reynolds, Ch. 11, Applied Science Publishers, Ltd., London (1979).
20. L. R. G. Treloar, "The Physics of Rubber Elasticity," Ch. 5, Clarendon Press, Oxford (1975).
21. D. J. Buckley, Paper presented at Rubber Division, A. C. S., May, 1974.
22. A. Stevenson, *Int. J. Fracture*, **23**, 47 (1983).